Distillation of mixed-state continuous-variable entanglement by photon subtraction

Sheng Li Zhang and Peter van Loock[*]

*Optical Quantum Information Theory Group, Max Planck Institute for the Science of Light, Günther-Scharowsky-Str. 1/Bau 26,
D-91058 Erlangen, Germany and Institute of Theoretical Physics I, Universität Erlangen-Nürnberg, Staudstr. 7/B2,
D-91058 Erlangen, Germany*

We present a detailed theoretical analysis for the distillation of one copy of a mixed two-mode continuous-variable entangled state using beam splitters and coherent photon-detection techniques, including conventional on-off detectors and photon-number-resolving detectors. The initial Gaussian mixed-entangled states are generated by transmitting a two-mode squeezed state through a lossy bosonic channel, corresponding to the primary source of errors in current approaches to optical quantum communication. We provide explicit formulas to calculate the entanglement in terms of logarithmic negativity before and after distillation, including losses in the channel and the photon detection, and show that one-copy distillation is still possible even for losses near the typical fiber channel attenuation length. A lower bound for the transmission coefficient of the photon-subtraction beam splitter is derived, representing the minimal value that still allows to enhance the entanglement.

I. INTRODUCTION

Entanglement of composite systems represented by continuous quantum variables is of conceptual importance for studying fundamental questions of quantum mechanics [1] and promises to be useful for potential real-world applications in the fast-developing field of quantum information processing [2–4]. However, in general, entanglement is a fragile resource which is easily degraded when it interacts with an uncontrollable environment, for example, in a communication channel in form of a lossy and noisy, optical fiber. In order to overcome this problem of entanglement degradation, typically, protocols such as entanglement purification or distillation will be utilized, as originally proposed for qubits [5]. These schemes detect errors and are usually probabilistic, as opposed to deterministic approaches such as quantum error correction. More generally, entanglement distillation can be defined as any scheme that creates one or more entangled pairs of higher entanglement from one or more copies of initially imperfectly entangled pairs by means of local operations and classical communication.

Although many impressive experiments for the distillation of pure or mixed discrete-variable entanglement have been reported [6–9], distilling continuous-variable entanglement appears to differ rather significantly and, in general, is harder to achieve. The difficulty arises mainly from the necessity of a non-Gaussian element for distilling Gaussian entangled states [10–12]. For instance, in order to distill the quantum optical two-mode squeezed state (TMSS) whose quadratures obey Gaussian statistics, one must introduce at least one non-Gaussian operation, in the form of a non-Gaussian ancilla or a non-Gaussian measurement. The so-called photon subtraction (PS) strategy, first introduced by Opatrný *et al.* [13], is one of the experimentally most readily available operations beyond the Gaussian regime. It enables one to modify the Gaussian statistics of a given TMSS and therefore serves as a possible approach to entanglement distillation of such Gaussian states [14]. The basic principle of the PS technique is very simple and can be implemented using beam splitters and photon measurements.

After Opatrný *et al.*'s pioneering work [13], many efforts have been made to improve the performance of such an entanglement distillation protocol. Olivares *et al.* [15] proposed an inconclusive PS method, which employs a more realistic on-off photon detector in order to enhance the entanglement. Kitagawa *et al.* [16] presented a fairly complete theoretical analysis of this type of distillation, including a numerical evaluation of the entanglement before and after distillation. Moreover, a multimode theory for frequency mode matching in the photon-subtracting operation was derived [17]. Even an experiment implementing Opatrný's method has already been reported [18]. These efforts, both on the theoretical and the experimental side, are examples for the more recent attempts to combine discrete-variable and continuous-variable approaches to optical quantum information processing [19].

The original scheme by Opatrný *et al.* as well as its theoretical refinements and extensions all refer to a single copy of a *pure*, Gaussian entangled state which is distilled into a non-Gaussian entangled state. This kind of distillation is sometimes referred to as entanglement concentration, distinct from entanglement purification protocols in which initially mixed-entangled states are purified and thereby turned into states with higher entanglement. Even though usually such entanglement purification is applied to two or more copies of entangled states [5], one mixed-entangled copy may also be distilled through local, generalized measurements, similar to those for concentrating a single pure-state copy into a maximally entangled state [20–23]. In the mixed-state case, however, both parties sharing the initial state must perform local measurements and communicate their results.

In this article, we provide a detailed analysis for the one-copy distillation of *mixed* continuous-variable entanglement, using beam splitters and experimentally feasible photon detection techniques. In other words, similar to those one-copy schemes mentioned in the preceding paragraph, we shall

---

[*]peter.vanloock@mpl.mpg.de

consider non-Gaussian, generalized measurements locally performed on the two modes of the initial Gaussian state. Note that PS ideally corresponds to maps like $\hat{a}|n\rangle = \sqrt{n}|n-1\rangle$ or $\hat{a}|\alpha\rangle = \alpha|\alpha\rangle$, with the photon annihilation operator being nonunitary and the resulting states being not normalized—a manifestation of the probabilistic nature of the PS process. The corresponding generalized measurements are realized through beam-splitter transformations, locally acting on the two signal modes and additional ancilla vacuum modes, and subsequent photon measurements. Note that various experiments have already demonstrated how versatile PS is for non-Gaussian state engineering [24–26]. Local filters for entanglement concentration of one copy of a pure TMSS were previously considered using Kerr interactions or cavity-QED [27]. Multicopy distillations of noisy versions of a TMSS have been proposed as well [28–30].

A further recent one-copy scheme for distilling mixed continuous variable entanglement was proposed in Ref. [31]. Differing from our analysis, this proposal [31] employs detections of collective excitations in atomic ensembles for the non-Gaussian operations. Further, it uses only operational entanglement measures, namely teleportation fidelities. Here, we shall calculate both fidelities and, in particular, logarithmic negativities for the distilled states.

While in the theoretical analysis of Ref. [16], the initial states are pure (and become mixed only for the case of on-off detections), the input states of the recent experiment [18] were mixed due to experimental imperfections such as the complication to prepare a perfectly pure, minimum-uncertainty squeezed state. Although even the idealized pure-state versions of that experiment slightly differ from the TMSSs used in our analysis (by local squeezing operations), the present article also provides a more general theoretical foundation of the experiment described in Ref. [18]. It proves the possibility and feasibility of realistic PS-based distillation of a TMSS, even in the presence of high losses. At the same time it illuminates the applicability of Opatrný's PS distillation protocol [13] and provides more details on how to improve entanglement in a general, realistic mixed-state scenario; for instance, in optical quantum communication using lossy fibers of nearly one attenuation length as potentially used in a quantum repeater [32]. Moreover, some of our results are fully analytical, thus further extending the theory presented in Ref. [16].

The article is organized as follows. First, in Sec. II, we will give a description of our scheme for entanglement distillation, along with the method for generating of our mixed entangled state. In Sec. III, the definition of logarithmic negativity is briefly summarized. With such a figure of merit for entanglement, the amount of entanglement before distillation is explicitly derived. Section IV is devoted to the entanglement distillation with conventional on-off detectors. An exact analytical formula for the entanglement distillation of pure TMSSs is obtained, which previously was only numerically investigated by Kitagawa *et al.* [16]. In Sec. V, we discuss two different strategies of applying photon-number-resolving detectors [pure and mixed photon-number-resolving (PNR)]. The success probability of distillation and the corresponding lower bounds T_L are studied, respectively. In Sec. VI, to further illustrate our results, we calculate an operational measure of entanglement (the fidelity in quantum teleportation), leading

to yet another way to compare the entangled states before and after distillation. Finally, we conclude with a discussion and summary in Sec. VII.

II. LOSSY BOSONIC CHANNEL AND PHOTON SUBTRACTION

Let us first introduce the amplitude-damped TMSS with which we are mainly concerned in this article. This kind of mixed-state entanglement can be obtained by sending each mode of a pure TMSS through a lossy bosonic channel. In our theoretical analysis, we shall simulate the lossy channel through an extra vacuum mode and a beam splitter. This is the simplest model for mimicking realistic fiber-optical light propagation, where more and more signal photons are gradually absorbed on the way during the channel transmission.

The entire scheme for our distillation protocol is shown in Fig. 1. The initial pure TMSS is given by

$$|\psi\rangle_{AB} = \sum_{n=0}^{\infty} \alpha_n |n\rangle_A |n\rangle_B, \alpha_n = \sqrt{1-\lambda^2}\lambda^n, \quad (1)$$

with $\lambda = \tanh(r)$ representing the degree of squeezing and A, B referring to the two transmitted modes. Two beam splitters with transmission coefficient $T_0 = \eta$ and auxiliary vacuum modes E, F are put into the ideal channels in order to simulate two lossy channels with transmission efficiency η. The PS-based distillation is implemented using two more beam splitters (each with transmission T) and photon detectors. Due to the finite reflectance of these beam splitters, the photon subtraction process heralded by the photon detectors is a probabilistic process and successful distillation may occur whenever both detectors register nonzero counts.

To give a systematical analysis, in this article, we shall consider entanglement distillation with two different types of detectors, namely conventional on-off detectors (e.g., avalanche photodiodes, APD) and PNR detectors, both of which are widely used in quantum optical experiments.
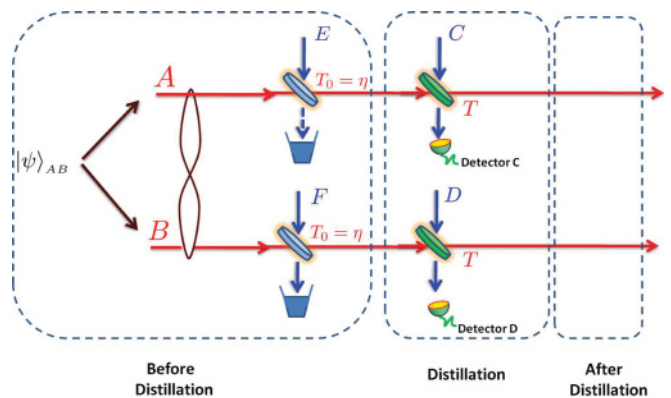
FIG. 1. (Color online) Scheme of continuous-variable entanglement distillation. The initial state $|\psi\rangle_{AB}$ is a pure two-mode squeezed vacuum state, both beams of which are transmitted through beam splitters with transmittance $T_0 = \eta$ in order to simulate a lossy bosonic channel of transmission η. The beam splitters with transmittance T including the photon detectors are used to achieve the photon subtractions for entanglement distillation. The input states of the C, D, E, F modes are pure vacuum states. An event of successful distillation is heralded when both detectors register nonzero counts.

III. LOGARITHMIC NEGATIVITY AND ENTANGLEMENT BEFORE DISTILLATION

Following the definitions of Ref. [16], we will use the logarithmic negativity as a figure of merit to quantify entanglement. The logarithmic negativity [33–35] is a relatively easily computable measure of entanglement; more precisely, it is an entanglement monotone, both under local operations and classical communication and under positive partial transpose preserving operations.

The *logarithmic negativity* of a bipartite state $\rho_{AB} = \rho$ is defined by

$$E_N(\rho) = \log_2[1 + 2N(\rho)], \tag{2}$$

in which $N(\rho)$ is defined as the *negativity* given by the absolute value of the sum of negative eigenvalues of the partially transposed density operator ρ^{Γ_A}. Here and throughout, without loss of generality, we will perform the partial transpose operation with respect to the A mode.

We shall now quantify the amount of entanglement of the amplitude-damped TMSS. Note that this state including the damping effect remains a Gaussian state, and hence its logarithmic negativity could be directly computed from its second-moment covariance matrix through the corresponding symplectic eigenvalues of the partially transposed state [2–4]. However, for our purposes, since the PS process will lead to non-Gaussian states, it is more useful to achieve a more general entanglement quantification expressed in the photon number basis. This is similar to the approach of Ref. [16], but with the important distinction that our states are mixed states from the beginning, both before and after the distillation.

First, let us denote the beam-splitter coupling between modes k and l as [16],

$$V_{kl}(\theta_0) = \exp[\theta_0(a_k^\dagger a_l - a_k a_l^\dagger)], \tag{3}$$

with $\theta_0 = \arctan(\sqrt{(1-\eta)/\eta})$ and $a_{k(l)}$ being the photon annihilation operator of the $k(l)$ mode. The unitary state evolution before entanglement distillation can be formulated as follows,

$$|\Psi\rangle_{ABEF} = V_{AE}(\theta_0) \otimes V_{BF}(\theta_0)|\psi\rangle_{AB}|0\rangle_E|0\rangle_F, \tag{4}$$

where $|0\rangle_E, |0\rangle_F$ are the initial vacuum states of the loss modes. Through direct calculation, we have

$$|\Psi\rangle_{ABEF} = \sum_{n=0}^\infty \sum_{k,l=0}^n \alpha_n \xi_{nk}\xi_{nl}|n-k\rangle_A|n-l\rangle_B|k\rangle_E|l\rangle_F,$$
$$\tag{5}$$
$$\xi_{nm} = (-1)^m\sqrt{\binom{n}{m}}(\sqrt{\eta})^{n-m}(\sqrt{1-\eta})^m,$$

where $m = 0,1,\ldots,n$ and $\binom{n}{m} = \frac{n!}{m!(n-m)!}$ is the binomial coefficient.

The mixed state ρ_{AB} before entanglement distillation is obtained by tracing over the loss modes E and F,

$$\rho_{\text{mix}} \equiv \rho_{AB} = \text{Tr}_{EF}[|\Psi\rangle_{ABEF}\langle\Psi|]$$
$$= \sum_{m,n=0}^\infty \sum_{i=0}^n \sum_{j=0}^m f_{nmij}|n-i\rangle_A\langle m-i|$$
$$\otimes |n-j\rangle_B\langle m-j|, \tag{6}$$

with f_{nmij} being a real positive coefficient, $f_{nmij} = \alpha_n\alpha_m\xi_{ni}\xi_{mi}\xi_{nj}\xi_{mj}$.

Similarly to the case of a pure TMSS [16,36], the partial transpose of the density matrix (6) is still block diagonal in the photon number (Fock) basis. We have

$$\rho_{AB}^{\Gamma_A} = \sum_{m,n=0}^\infty \sum_{i=0}^n \sum_{j=0}^m f_{nmij}|m-i,n-j\rangle_{AB}\langle n-i,m-j|$$
$$= \bigoplus_{K=0}^\infty \sum_{i,j=0}^K C_{i,j}^{(K)}|i,K-i\rangle_{AB}\langle j,K-j|, \tag{7}$$

with

$$C_{i,j}^{(K)} = (1-\lambda^2)\left(\frac{\eta}{1-\eta}\right)^K \sum_{n=n_0}^\infty \sqrt{\binom{K}{i}\binom{K}{j}}$$
$$\times (\lambda - \lambda\eta)^{(i+j+2n)}\frac{(n+i)!(n+j)!}{K!n!(n+i+j-K)!}, \tag{8}$$

$$n_0 = \max\{0, K-i-j\}.$$

Thus, the negativity of ρ_{mix} can be equivalently obtained by solving the eigenvalue problem of a series of $(K+1)\times(K+1)$ submatrices

$$\mathbf{C}_K = \left[C_{i,j}^{(K)}\right]_{i=0,\ldots,K;j=0,\ldots,K}, \tag{9}$$

for $K = 0,1,\ldots,\infty$. Such a block submatrix method is quite efficient in numerical evaluations [16]. Indeed, the matrix $\mathbf{C}_K$ has a very useful symmetry property which will finally simplify the whole problem.

Theorem 1. $\mathbf{C}_K$ is a double symmetric, i.e., both symmetric and centrosymmetric, matrix.

Proof. Symmetric property follows directly from the i,j exchange invariance in the definition Eq. (8). Therefore we only need to prove $C_{i,j}^{(K)} = C_{K-i,K-j}^{(K)}$ for arbitrary i,j. Now consider any i,j such that for $i+j \leqslant K$, we always have $(K-i) + (K-j) \geqslant K$. Using Eq. (8), it directly follows $n_0(i,j) = K-i-j \geqslant 0$ and $n_0(K-i,K-j) = 0$. By replacing the index $n = n' + n_0(i,j)$ in the summation of $C_{i,j}^{(K)}$ and noticing $\binom{K}{i} = \binom{K}{K-i}$, the relation $C_{i,j}^{(K)} = C_{K-i,K-j}^{(K)}$ can be straightforwardly obtained. ∎

Theorem 2. The negativity of ρ_{mix} can be uniquely determined by the skew diagonal entries of matrix $\mathbf{C}_K$:

$$N(\rho_{\text{mix}}) = \frac{1}{2}\left(\sum_{K=0}^\infty \text{Tr}[\mathbf{J}_K\mathbf{C}_K] - 1\right), \tag{10}$$

with $\mathbf{J}_K$ being the anti-identity matrix,

$$\mathbf{J}_K = [\delta_{i+j,K}]_{i,j=0,\ldots,K} = \begin{pmatrix} 0 & 0 & \cdots & 0 & 1 \\ 0 & 0 & \cdots & 1 & 0 \\ \vdots & \vdots & \ddots & \vdots & \vdots \\ 0 & 1 & \cdots & 0 & 0 \\ 1 & 0 & \cdots & 0 & 0 \end{pmatrix}. \tag{11}$$

Proof. According to Ref. [37], for a $(K+1)\times(K+1)$ dimensional matrix $\mathbf{C}_K$, there always exists an orthogonal matrix U, such that for K odd,

$$U\mathbf{C}_K U^T = \begin{pmatrix} A - JM & 0 \\ 0 & A + JM \end{pmatrix}, \tag{12}$$

and for K even,

$$UC_KU^T = \begin{pmatrix} A - JM & 0 & 0 \\ 0 & q & \sqrt{2}x^T \\ 0 & \sqrt{2}x & A + JM \end{pmatrix}, \quad (13)$$

where A, M, and J are each $\lfloor \frac{K+1}{2} \rfloor \times \lfloor \frac{K+1}{2} \rfloor$ matrices with elements

$$A_{i,j} = C_{i,j}^{(K)}, \quad M_{i,j} = C_{i+\lceil \frac{K-1}{2} \rceil, j}^{(K)}, \quad J_{i,j} = \delta_{i+j, \lfloor \frac{K-1}{2} \rfloor},$$

for $i, j = 0, 1, \ldots, \lfloor (K-1)/2 \rfloor$, and $\lfloor \cdots \rfloor$ and $\lceil \cdots \rceil$ are the floor and ceiling functions, respectively.

This shows that the eigenvalues of $\mathbf{C}_K$ are the same as the eigenvalues of $A - JM$ and $A + JM$ in the case of K odd and the same as $A - JM$ and $\begin{pmatrix} q & \sqrt{2}x^T \\ \sqrt{2}x & A+JM \end{pmatrix}$ in the case of K even.

Moreover, it can be always checked that the sub-block $A - JM$ contains all the negative eigenvalues of matrix $\mathbf{C}_K$. In fact, for the matrix $\mathbf{C}_K$ as defined in Eq. (8), $A - JM$ is always negative-definite, whereas the sub-block $A + JM$ and $\begin{pmatrix} q & \sqrt{2}x^T \\ \sqrt{2}x & A+JM \end{pmatrix}$ are positive-definite. Thus, the absolute value of the sum of the negative eigenvalues of $\mathbf{C}_K$ is given by $|\text{Tr}[A - JM]| = \text{Tr}[JM - A] = \frac{1}{2}\text{Tr}[\mathbf{J}_K\mathbf{C}_K - \mathbf{C}_K]$. The negativity of the whole matrix ρ_{mix} follows as

$$N(\rho_{\text{mix}}) = \frac{1}{2} \sum_{K=0}^{\infty} \text{Tr}[\mathbf{J}_K\mathbf{C}_K - \mathbf{C}_K]$$
$$= \frac{1}{2} \left(\sum_{K=0}^{\infty} \text{Tr}[\mathbf{J}_K\mathbf{C}_K] - 1 \right), \quad (14)$$

where in the second line, we have imposed the normalization condition

$$\sum_{K=0}^{\infty} \text{Tr}[\mathbf{C}_K] = \text{Tr}(\rho_{AB}^{\Gamma_A}) = \text{Tr}(\rho_{AB}) = 1. \quad (15)$$

∎

Thus, following the definition in Eq. (2), the logarithmic negativity of the state in Eq. (6) can now be easily calculated as

$$E_N(\rho_{\text{mix}}) = \log_2 \left(\sum_{K=0}^{\infty} \text{Tr}[\mathbf{J}_K\mathbf{C}_K] \right)$$
$$= \log_2 \frac{1+\lambda}{1 - \lambda(2\eta - 1)}. \quad (16)$$

By setting $\eta = \exp(-\gamma t)$, our result agrees with that presented in Ref. [36]; however, our derivation leads to a simple, closed expression as a function of the input squeezing and channel loss. For this still Gaussian state before distillation, we can also confirm our result by calculating the symplectic eigenvalues of the partially transposed state.

Following our formalism above, we merely need to calculate the skew diagonal entries $\{C_{i,K-i}^{(K)}\}_{i=0,\ldots,K}$ in order to obtain the logarithmic negativity for the two-mode mixed entangled state. It is important to note that Theorem 1 and Theorem 2 can also be applied to calculate the logarithmic negativity after entanglement distillation. In fact, PS on both transmitted

modes does not change the symmetry and centrosymmetry of the partially transposed density matrix $\rho_{AB}^{\Gamma_A}$, provided that *both detectors obtain the same measurement results*. The only difference is that the state after PS is not normalized. One should then specify the normalization factor (i.e., the trace of $\rho_{AB}^{\text{dist}} = \sum_K \text{Tr}[\mathbf{C}_K]$) for the different types of detectors and the different detection strategies. This enables us to extend the analytical formulas for continuous-variable entanglement from pure states to mixed states, including the Gaussian state ρ_{mix} before distillation as well as the non-Gaussian states after distillation using on-off detectors or PNR detectors (in pure and mixed strategies, see below).

IV. DISTILLATION USING ON-OFF DETECTION

For convenience, let us first give a general description of photon detectors. Suppose the detector can respond with $\mathcal{M}$ different measurement outcomes. According to the theory of generalized quantum measurements [38,39], such a measurement device can be completely characterized through a set of positive-definite operators $\{\hat{\Pi}_k | k = 1, 2, \ldots, \mathcal{M}\}$, corresponding to a positive operator-valued measure (POVM). The quantum measurement is probabilistic: for a given input state ϱ, the probability that the detector gives outcome k is $P_k = \text{Tr}[\hat{\Pi}_k\varrho]$. The condition that the total probability is normalized corresponds to $\sum_{k=1}^{\mathcal{M}} \hat{\Pi}_k = \mathbb{1}$, with $\mathbb{1}$ representing the identity operator.

The photon detectors usually employed in quantum optical experiments, such as APD operating in the Geiger mode, correspond to a measurement device with only two measurement outcomes: off (no photons detected) and on (one or more photons detected). Expressed in the Fock basis, the positive operator description of an ideal on-off photon detector is then given by $\{\hat{\Pi}^{(\text{off})}, \hat{\Pi}^{(\text{on})}\}$, with

$$\hat{\Pi}^{(\text{off})} = |0\rangle\langle 0|,$$
$$\hat{\Pi}^{(\text{on})} = \mathbb{1} - \hat{\Pi}^{(\text{off})} = \sum_{k=1}^{\infty} |k\rangle\langle k|. \quad (17)$$

Based on the formalism and the notations above, we can now proceed with the entanglement distillation protocol in Fig. 1. Assuming that the two beam splitters for PS have the same transmittance T (reflectance coefficient $R = 1 - T$), the state evolution of the whole PS process can be described by

$$\rho_{ABCD} = \mathbb{V}[\rho_{\text{mix}} \otimes |0\rangle_C\langle 0| \otimes |0\rangle_D\langle 0|]\mathbb{V}^\dagger,$$
$$\widetilde{\rho}(\text{on,on}) = \frac{\text{Tr}_{CD}[\rho_{ABCD}\mathbb{1}_{AB} \otimes \hat{\Pi}_C^{(\text{on})} \otimes \hat{\Pi}_D^{(\text{on})}]}{P(\text{on,on})}, \quad (18)$$

where $\mathbb{V} = V_{AC}(\theta) \otimes V_{BD}(\theta)$, $\theta = \arctan(\sqrt{R/T})$, and $\widetilde{\rho}(\text{on,on})$ is the normalized output state; $P(\text{on,on})$ is the probability of detecting nonzero photons in both detectors,

$$P(\text{on,on}) = \text{Tr}[\rho_{ABCD}\mathbb{1}_{AB} \otimes \hat{\Pi}_C^{(\text{on})} \otimes \hat{\Pi}_D^{(\text{on})}], \quad (19)$$

where this time the trace is over all four modes ABCD. Using the same method as in Sec. III, analytic formulas for the entanglement and the success probability can now be

derived. The unnormalized, partial transpose $\rho_{AB}^{\Gamma_A}$ is again block diagonal with respect to the K subspaces. We have

$$C_{i,j}^{(K)}(\text{on,on}) = (1 - \lambda^2)\left(\frac{\eta T}{1-\eta}\right)^K \sum_{\gamma=1}^{\infty}\sum_{\delta=1}^{\infty}$$

$$\times \sum_{n=n_0}^{\infty}\left(\frac{\eta R}{1-\eta}\right)^{\gamma+\delta}(\lambda - \lambda\eta)^{i+j+2n+2\gamma}$$

$$\times \frac{(i+n+\gamma)!(j+n+\gamma)!}{K!n!\gamma!\delta!(n+i+j+\gamma-K-\delta)!}$$

$$\times \sqrt{\binom{K}{i}\binom{K}{j}},$$

$$n_0 = \max\{0, K+\delta-i-j-\gamma\}. \qquad (20)$$

The probability of success can be evaluated as

$$P(\text{on,on}) = \sum_{K=0}^{\infty}\sum_{i=0}^{K} C_{i,i}^{(K)}(\text{on,on})$$

$$= \frac{\lambda^2(1-\widetilde{T})^2(1+\lambda^2\widetilde{T})}{(1-\lambda^2\widetilde{T})(1-\lambda^2\widetilde{T}^2)}, \qquad (21)$$

where we define $\widetilde{T} = 1 - \eta R$ and $\widetilde{R} = 1 - \eta T$.

After state normalization, the logarithmic negativity can be also analytically obtained:

$$E_N(\widetilde{\rho}(\text{on,on})) = \log_2\left[\frac{(1-\lambda^2)\eta R}{(1-\lambda\eta T)^2 - \lambda^2(1-\eta)\widetilde{R}}\right]$$

$$+ \log_2\left[\frac{\widetilde{R}}{(1-\lambda)(1-\lambda(2\eta T - 1))}\right]$$

$$- \frac{1-\eta}{(1-\lambda\eta T)^2 - \lambda^2(1-\eta)^2}\right]$$

$$+ \log_2\left[\frac{(1-\lambda^2\widetilde{T})(1-\lambda^2\widetilde{T}^2)}{(1-\widetilde{T})^2(1+\lambda^2\widetilde{T})}\right]. \quad (22)$$

In the following discussions, to be more specific, we shall choose two typical values for the channel transmission η in order to study the entanglement properties after distillation.

A. Pure TMSS: $\eta = 1$

In the literature, PS-based distillation of a pure TMSS has already been numerically treated in Ref. [16]. In that work, due to the extremely intensive numerical computation for diagonalizing a large square matrix, only the low-squeezing regime $\lambda < 0.9$ was investigated and high photon number terms were neglected. However, based on our *analytical* result in Eq. (22), the performance of entanglement distillation in the large-squeezing (high photon number) regime $0.9 < \lambda < 1.0$ can also be examined.

In fact, by simply setting $\eta = 1$, we obtain

$$E_N(\widetilde{\rho})_{\eta=1} = \log_2\left[\frac{(1+\lambda)(1-\lambda^2 T)(1+\lambda T)}{(1-\lambda T)(1+\lambda^2 T)(1-\lambda T+\lambda R)}\right], \qquad (23)$$

$$P(\text{on,on})_{\eta=1} = \frac{\lambda^2(1-T)^2(1+\lambda^2 T)}{(1-\lambda^2 T)(1-\lambda^2 T^2)}. \qquad (24)$$

Surprisingly, for a given beam splitter with finite transmission coefficient $0 < T < 1$, the output entanglement exhibits nonmonotonic dependence of the initial squeezing parameter λ. The finite transmission coefficient of the beam splitter has a degrading effect on the output entanglement. When $\lambda \to 1$, a pure TMSS has infinite entanglement. However, when one uses the beam splitter together with on-off detectors to implement the distillation, one will always get finite entanglement. In fact, the optimal squeezing parameter λ (referred to as λ_{opt}) which maximizes $E_N(\widetilde{\rho})$ is strictly smaller than 1. This result is certainly of experimental significance in order to optimize the distilled entanglement: it may not be necessary to prepare as much initial squeezing as possible to maximize the final entanglement; some finite-squeezing value will be optimal.

In Fig. 2(a), we show the logarithmic negativity of the distilled TMSS ($\eta = 1$) for different beam-splitter transmissions ($T = 0.1, 0.5, \ldots, 0.99$). In Fig. 2(b), we give a plot of the probability of successful distillation, $P(\text{on,on})$. Figure 2(c) shows the optimal λ_{opt} as a function of T, while Fig. 2(d) presents the maximal $E_N(\widetilde{\rho})$ at $\lambda = \lambda_{\text{opt}}$. Even with infinite squeezing and a nonlossy channel, $\eta = 1$, we cannot approach infinite entanglement after distillation. In fact, when $\lambda \to 1$, in Eq. (23), the logarithmic negativity scales as $E_N(\widetilde{\rho}) = \log_2\frac{1}{1-T}$.

In the above distillation protocol, there exists a nontrivial lower bound T_L for the transmission coefficient T below which the PS scheme based on beam splitters and on-off detectors ceases to improve the entanglement. In Fig. 2(a), it is shown that the distillation protocol effectively no longer works for $T = 0.10, 0.50$. The entanglement after distillation is then even smaller than that before distillation. Indeed, requiring $E_N(\widetilde{\rho}) > E_N(\rho_{\text{mix}})$, the transmission coefficient T satisfies $T_L < T \leqslant 1$, with

$$T_L = \frac{1}{3\lambda^3}\left[\lambda(\lambda^2 + \lambda - 1) + 2\sqrt{\xi}\sin\left(\frac{\pi}{6} - \frac{\tilde{\theta}}{3}\right)\right],$$

$$\xi = \lambda^2(\lambda^4 + 2\lambda^3 - 4\lambda^2 + 4\lambda + 1),$$

$$\zeta = \lambda(\lambda^3 + 8\lambda^2 - 3\lambda + 2),$$

$$\tilde{\theta} = \arccos\left(\frac{3\lambda^3\zeta - 2\lambda(\lambda^2 + \lambda - 1)\xi}{2\xi\sqrt{\xi}}\right). \qquad (25)$$

The quantity T_L in Eq. (25) is a monotonically increasing function of the squeezing parameter λ. When $\lambda \to 0$, we have $T_L = 1/2$. In the other extreme case, when λ approaches 1, it follows that $T_L \to 1$. This, on the other hand, proves the degrading effect of the transmission coefficient T: In the high photon number regime (especially, for $\lambda \to 1$), any finite transmission $0 < T < 1$ is smaller than $T_L = 1$ and the entanglement of the state after distillation, as illustrated in Fig. 1, is finite and hence smaller than the infinite entanglement before distillation. We give a detailed description of the behavior of T_L in Fig. 4.

B. 3-dB amplitude-damped TMSS: $\eta = 0.5$

In Fig. 3, we show the success probability and the logarithmic negativity of the amplitude-damped TMSS. Here, the amplitude-damping process is simulated by a 3-dB beam splitter: $\eta = 1/2$. Similarly to the distillation of a pure TMSS, the entanglement of the distilled state including amplitude
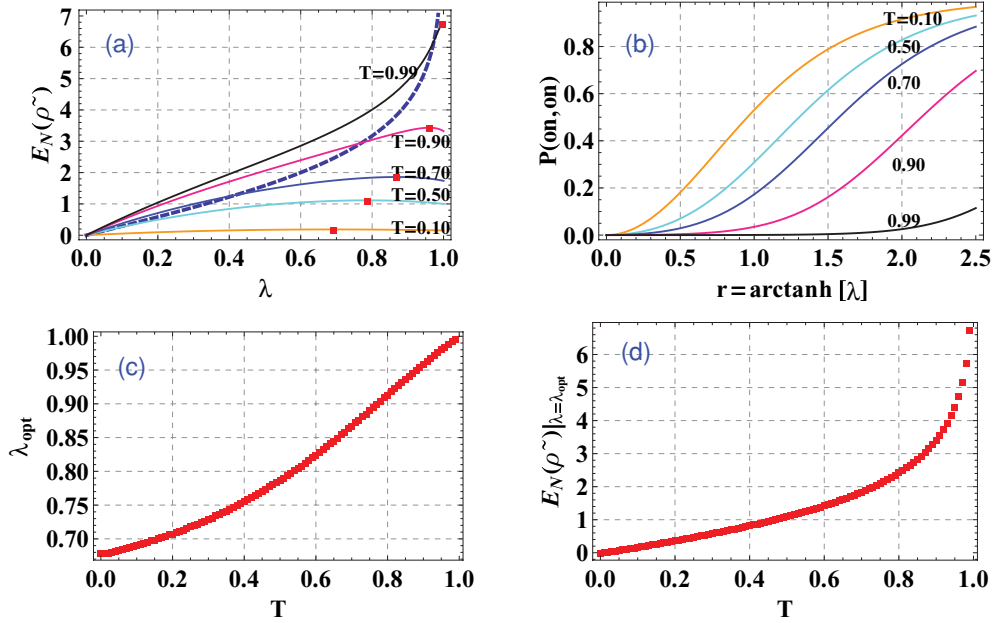
FIG. 2. (Color online) Performance of distilling a pure TMSS ($\eta = 1$) with beam splitters and on-off detectors. (a) Logarithmic negativity of the output state for $T = 0.10, 0.50, 0.70, 0.90, 0.99$, respectively. The dashed line corresponds to the logarithmic negativity of the TMSS before distillation [Eq. (16) with $\eta = 1$]. The red squares in each curve indicate the maximum values of $E_N(\tilde\rho)$. (b) Success probability, i.e., the probability that both detectors record the "on" results [Eq. (24)]. (c) λ_{opt} as a function of T (see text for more information). (d) Maximal value of $E_N(\tilde\rho)$ at $\lambda = \lambda_{\mathrm{opt}}$.

damping is again degraded by the finite transmission coefficient. There also exists a finite λ_{opt} with $0 < \lambda_{\mathrm{opt}} < 1$ which maximizes the output entanglement. At the same time, the lower bound T_L for the transmission coefficient still increases monotonically from $T_L = 1/2$ to $T_L = 1$, when λ varies from 0 to 1.

In Fig. 4, we show a plot to describe the relation between T_L and λ, for η varying from 0.01 to 1. It is shown that for larger channel losses (smaller η), more transmissive beam splitters (larger T) are needed in order to achieve distillation. Furthermore, for all $0 < \eta \leqslant 1$, the values T_L vary from $1/2$ to 1, which means a beam-splitter transmission $T > 1/2$ is a
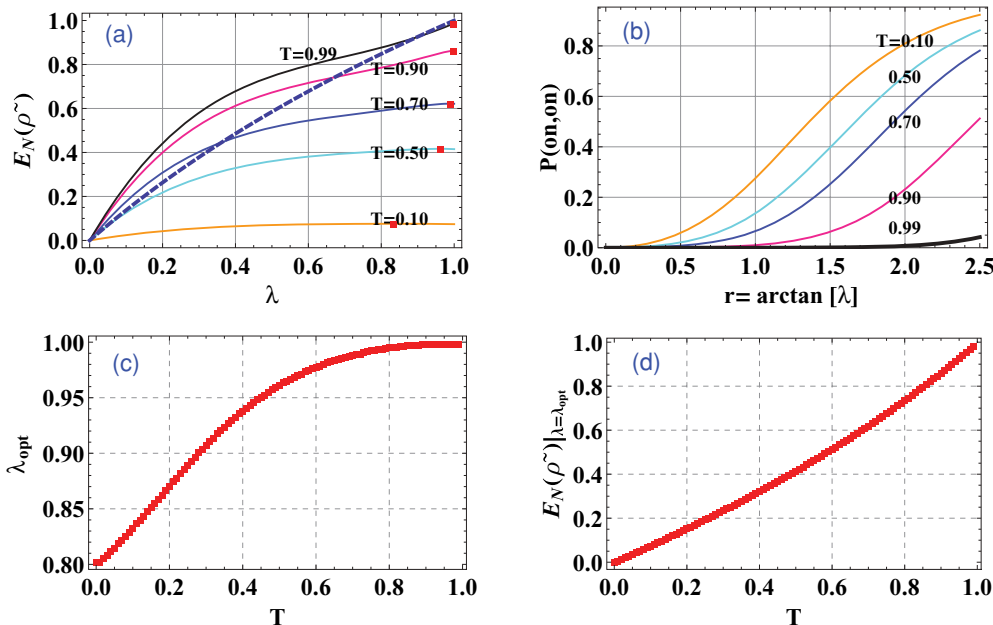
FIG. 3. (Color online) Performance of distilling a 3-dB amplitude-damped TMSS ($\eta = 1/2$) with beam splitters and on-off detectors. (a) Logarithmic negativity of the output state for $T = 0.10, 0.50, 0.70, 0.90, 0.99$, respectively. The dashed line corresponds to the logarithmic negativity of the amplitude-damped TMSS before distillation [Eq. (16)]. The red squares indicate the maximum values of $E_N(\tilde\rho)$. (b) Success probability of distillation for various T [Eq. (24)]. (c) λ_{opt} as a function of T. (d) Maximal value of $E_N(\tilde\rho)$ at $\lambda = \lambda_{\mathrm{opt}}$.
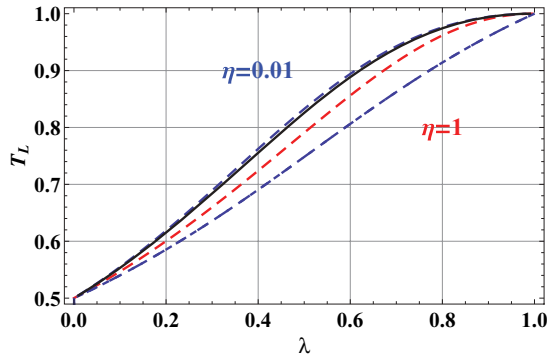
FIG. 4. (Color online) Lower bound T_L for distilling an amplitude-damped TMSS using beam splitters and on-off detectors. The channel transmissions η shown, from top to bottom, are $0.01, 0.1, 0.5, 1$. T_L increases monotonically with squeezing λ.

general, *necessary condition for distilling amplitude-damped TMSSs using on-off detectors.* However, in Sec. V, we will find that such a necessary condition can be circumvented by employing a more sophisticated detection strategy, for instance, using photon-number-resolving detectors.

V. DISTILLATION USING PHOTON NUMBER RESOLVING DETECTION

In quantum communication and computation, using photon-number-resolving detectors may lead to various important applications, such as linear-optics quantum computing

[40], quantum repeaters [41], quantum state discrimination [42], and quantum super-resolution [43]. Recently, a photon-number resolution of up to 10 photons was demonstrated [44]. In the following, we shall continue investigating PS-based entanglement distillation protocols, but we will replace the on-off detectors by PNR detectors. In our analysis, we will refer to two strategies: (i) pure PNR detection strategy and (ii) mixed PNR detection strategy.

A. Strategy 1: pure PNR detection

For simplicity, let us consider a perfect PNR detector which has a unique response for every input photon number state. The corresponding POVM operator for detecting ℓ photons is

$$\hat{\Pi}_\ell = |\ell\rangle\langle\ell|, \quad \sum_\ell^\infty \hat{\Pi}_\ell = \mathbb{1}. \tag{26}$$

This kind of measurement is pure in the sense that the operators $\hat{\Pi}_\ell$ ($\ell = 0, \ldots, \infty$) are extremal in the convex set of all POVMs. Now suppose both PNR detectors in Fig. 1 give the same photon number ℓ, then, according to Eq. (18), the output state can be written as

$$\widetilde{\rho}(\ell, \ell) = \frac{\text{Tr}_{CD}\left[\rho_{ABCD}\mathbb{1}_{AB} \otimes \hat{\Pi}_{\ell_C} \otimes \hat{\Pi}_{\ell_D}\right]}{P(\ell, \ell)}. \tag{27}$$

After direct calculation, we obtain the matrix elements of the partially transposed matrix $\rho_{A\bar{B}}^{\Gamma_A}$ (unnormalized) in the K subspace,

$$C_{i,j}^{(K)}(\ell, \ell) = (1 - \lambda^2)\left(\frac{\eta T}{1 - \eta}\right)^K \sum_{n=n_0}^{\infty} (\lambda \eta R)^{2\ell} (\lambda - \lambda\eta)^{i+j+2n} \sqrt{\binom{i+n+\ell}{n}\binom{j+n+\ell}{n}\binom{i+n+\ell}{i+j+n-k}\binom{j+n+\ell}{i+j+n-K}}$$

$$\times \sqrt{\binom{j+\ell}{\ell}\binom{i+\ell}{\ell}\binom{K-i+\ell}{\ell}\binom{K-j+\ell}{\ell}},$$

$$n_0 = \max\{0, K - i - j\}, \tag{28}$$

as well as the success probability,

$$P(\ell, \ell) = \frac{1 - \lambda^2}{1 - \lambda^2 \widetilde{T}^2}\left[\frac{\lambda \eta R}{1 - \lambda^2 \widetilde{T}^2}\right]^{2\ell} \sum_{k=0}^{\ell} \binom{\ell}{k}^2 (\lambda \widetilde{T})^{2k}. \tag{29}$$

The logarithmic negativity of the output state then becomes

$$E_N(\widetilde{\rho}(\ell, \ell)) = (2\ell + 1)\log_2\left[\frac{1 + \lambda \widetilde{T}}{1 - \lambda(\eta T + \eta - 1)}\right]$$

$$+ \log_2\left[\sum_{k=0}^{\ell} \binom{\ell}{k}^2 (\lambda - \lambda\eta)^{2k}(1 - \lambda\eta T)^{2\ell - 2k}\right]$$

$$- \log_2\left[\sum_{k=0}^{\ell} \binom{\ell}{k}^2 (\lambda \widetilde{T})^{2k}\right]. \tag{30}$$

In Fig. 5, we show the logarithmic negativity and the success probability for distilling a 3-dB amplitude-damped ($\eta = 1/2$) TMSS. The counted photon numbers are $\ell = 1, 2, 3, 4$. Compared with the distillation using on-off detectors, the PNR-based distillation has the following characteristics:

(i) For $\ell \geqslant 2$, the PNR detectors outperform the on-off detectors by a significant amount for small squeezing λ. The more photons are detected, the higher the entanglement will be. However, this improvement becomes negligible for large squeezing λ, for which the lower-bound T_L will be much greater than $T = 0.95$ (the value used in our calculation).

(ii) The success probability of the pure PNR distillation strategy decreases exponentially with the number of photons detected in each PNR detector, as can be seen in Eq. (29). As a consequence, the probability $P(\ell, \ell)$ is much smaller than the success probability $P(\text{on}, \text{on})$ for on-off detectors. To be more specific, we show a plot of $P(\ell, \ell)$ as a function
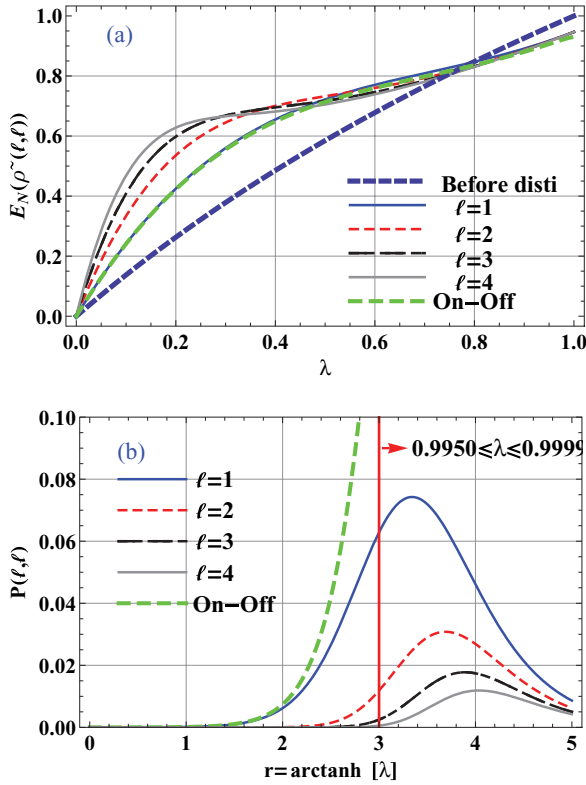
FIG. 5. (Color online) Comparison of the performance of entanglement distillation between PNR detectors (strategy 1) and on-off detectors. The green dashed lines correspond to the case of on-off detectors. The blue thick dashed lines in (a) represent the entanglement before distillation. Logarithmic negativity and success probability are shown for PNR detectors with counted photon numbers $\ell = 1,2,3,4$. The other parameters are set to $\eta = 1/2, T = 0.95$. The red arrow in (b) indicates the regime $0.9950 \leqslant \lambda \leqslant 0.9999$ $(3 \leqslant r \leqslant 5)$.

of $r = \text{arctanh}(\lambda)$ in Fig. 5(b). In the high-squeezing regime $(0.9950 \leqslant \lambda \leqslant 0.9999)(3 \leqslant r \leqslant 5)$, we observe a peak of $P(\ell,\ell)$. This is because larger squeezing results in more photons in each transmitted mode (A and B) and therefore leads to more photons to be detected by the PNR detectors. However, too large squeezing will shift the number of detected photons to a much higher level $\gg 4$, eventually decreasing the detection probability for the $\ell = 1,2,3,4$ photon number cases.

(iii) The lower-bound T_L for the transmittance of the beam splitter is shifted by the PNR detection results. In Fig. 6, we show T_L as a function of the number of photons detected, $\ell = 1,2,3,4$, and the channel efficiency, $\eta = 0.01, 0.1, 0.5, 1$. For $\ell = 1$, the bound T_L covers the full range between $1/2$ and 1, similarly to T_L for the on-off detection protocol (Fig. 4). For larger ℓ, e.g., $\ell = 2,3,4$, the minimum of T_L (at $\lambda = 0$) is independent of η and is shifted to $1/(\ell + 1)$, thus circumventing the necessary condition $T > 1/2$ for the on-off detection protocols.

B. Strategy 2: mixed PNR detection

To improve the probability of successful distillation, we introduce another distillation measurement strategy. This

time we shall still use photon number discrimination with PNR detectors, however, in a mixed PNR strategy. Such a strategy is experimentally more feasible than general pure PNR detections and similar experiments have already been reported in the context of binary coherent-state discrimination [42].

To achieve entanglement distillation, we make a postselection of the PNR detection results and define the POVM operators

$$\hat{\Pi}_{\text{on}}^{(m)} = \sum_{\ell \geqslant m}^{\infty} |\ell\rangle\langle\ell|, \quad \hat{\Pi}_{\text{off}}^{(m)} = \sum_{\ell=0}^{m-1} |\ell\rangle\langle\ell|. \quad (31)$$

Again, successful distillation is heralded when both PNR detectors record the "on" result. By taking into account the contribution of all multiphoton components $\ell \geqslant m$, the success probability approaches 1 in the case of infinite squeezing $(\lambda \to 1)$. For any m, we have

$$P_{\text{succ}}^{(m)} = \text{Tr}\big[\rho_{ABCD}\mathbb{1}_{AB} \otimes \hat{\Pi}_{\text{on}_C}^{(m)} \otimes \hat{\Pi}_{\text{on}_D}^{(m)}\big]$$

$$= (1 - \lambda^2) \sum_{n=m}^{\infty} \lambda^{2n} \left[1 - \sum_{k=0}^{m-1} \binom{n}{k}(\eta R)^k \widetilde{T}^{(n-k)}\right]^2. \quad (32)$$

When $m = 1$, such a strategy is straightforwardly reduced to the conventional on-off detection method in Sec. IV. However, for large m, the analytic formulas for success probability $P_{\text{succ}}^{(m)}$ and logarithmic negativity $E_N(\widetilde{\rho})$ become rather complicated and we shall only present a numerical comparison for different m values in Fig. 7. We still consider the typical example of 3-dB transmission $\eta = 1/2$ and highly transparent beam splitters, $T = 0.95$. As can been seen from Fig. 7(a), for smaller squeezing $\lambda < 0.5$ ($r < 0.5493$), a significant increase of entanglement is obtained. For larger squeezing $\lambda > 0.5$, the mixed PNR detection strategy does not improve the entanglement very much. The corresponding probability $P_{\text{succ}}^{(m)}$ is shown in Fig. 7(b).

Finally, in order to find out for which conditions this mixed-PNR protocol can improve entanglement, we also systematically vary the T values of the beam splitters and calculate the lower bound T_L [Fig. 7(c)]. Interestingly, the T_L bounds are similar to the pure-PNR case. For $\lambda \to 0$, a transmission of $T = 1/(m + 1)$ is sufficient to enhance the entanglement. However, as λ increases, our simulations suggest that a monotonically increasing T is required for successful distillation.

VI. OPERATIONAL MEASURE OF ENTANGLEMENT

In this section, we shall consider quantum teleportation of coherent states in order to assess the quality of the photon-subtracted entangled states. Quantum teleportation is a protocol in which an arbitrary, unknown quantum state can be reliably transferred from a sender to a receiver. The crucial resource for quantum teleportation to outperform classical teleportation is an entangled state shared by the two participants. Intuitively, the more entanglement they share, the higher the teleportation fidelity they can achieve. In other words, the teleportation fidelity may serve as an operational measure of entanglement [13,15].
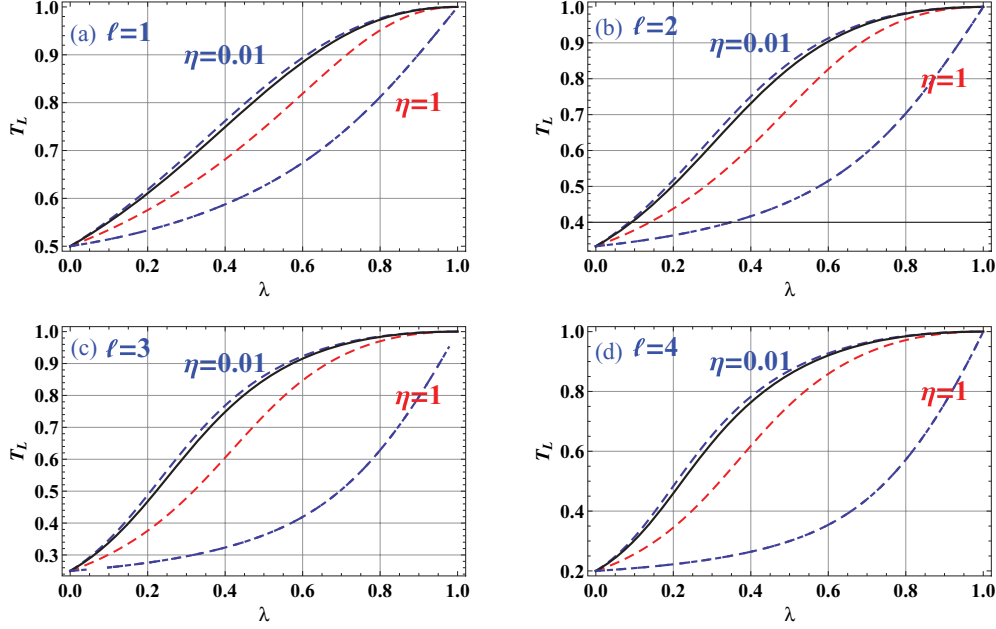
FIG. 6. (Color online) Lower-bound T_L for PNR-based distillation (strategy 1) of an amplitude-damped TMSS with the numbers of counted photons $\ell = 1, 2, 3, 4$. In each plot [(a)–(d)], the channel transmittance η is chosen to be $0.01, 0.1, 0.5, 1$, from top to bottom, and T_L ranges from $1/(\ell + 1)$ to 1.

In the following, we consider a teleportation experiment in which the entangled state after PS-based distillation is utilized. We assume that the state to be teleported is a coherent state, $\sigma_{in} = |\alpha\rangle\langle\alpha|$. Standard continuous-variable teleportation [45] consists of three steps: (i) Alice combines one mode of the entangled state, say the A mode, with the input mode in state σ_{in} at a 50:50 beam splitter; then she measures the quadratures variables $x_- = (x_{in} - x_A)/\sqrt{2}$ and $p_+ = (p_{in} + p_A)/\sqrt{2}$. (ii) When she obtains the classical measurement results for $\bar{x}_-$ and $\bar{p}_+$, she then communicates them to Bob via a classical communication channel. (iii) Using Alice's measurement results, Bob applies the corrsponding displacement operation $D(-\beta) = \exp(-\beta a_B^\dagger + \beta^* a_B), \beta = \bar{x}_- + i\,\bar{p}_+$ on the other entangled mode B. The fidelity between σ_{in} and the final state of mode B is related with the quality of the shared entanglement. Unit fidelity requires perfect entanglement.

Mathematically, the joint quadrature measurement on the input mode σ_{in} and mode A is equivalent to a heterodyne measurement (acting on mode A), expressible as [15]

$$\hat{\Pi}_A(\beta) = \frac{1}{\pi} D(\beta)\sigma_{in}^T D^\dagger(\beta), \quad (33)$$

where here T denotes the transposition operation. For the normalized entangled state $\widetilde{\rho}_{AB}$, the probability for outcome β is

$$P(\beta) = \text{Tr}[\widetilde{\rho}_{AB}\hat{\Pi}_A(\beta) \otimes \mathbb{1}_B]. \quad (34)$$

After the displacement operation by Bob, the final state in mode B becomes

$$\rho_B = \frac{1}{P(\beta)} D(-\beta)\text{Tr}_A[\widetilde{\rho}_{AB}\hat{\Pi}_A(\beta) \otimes \mathbb{1}_B]D^\dagger(-\beta), \quad (35)$$

with a fidelity given by

$$\begin{aligned} F_\beta &= \langle\alpha|\rho_B|\alpha\rangle \\ &= \frac{1}{P(\beta)}\langle\alpha + \beta|\text{Tr}_A[\widetilde{\rho}_{AB}\hat{\Pi}_A(\beta) \otimes \mathbb{1}_B]|\alpha + \beta\rangle. \end{aligned} \quad (36)$$

By averaging over all the possible measurement results β, we obtain the average fidelity

$$\begin{aligned} F &= \int d^2\beta\, P(\beta)F_\beta \\ &= \frac{1}{\pi}\int d^2\beta\,\text{Tr}[\widetilde{\rho}_{AB}D(\beta)\sigma_{in}^T D^\dagger(\beta) \otimes D(\beta)|\alpha\rangle\langle\alpha|D^\dagger(\beta)] \\ &= \text{Tr}[\widetilde{\rho}_{AB}\mathbf{O}_F], \end{aligned} \quad (37)$$

where we define the bipartite operator $\mathbf{O}_F = \frac{1}{\pi}\int d^2\beta\, D(\beta) \otimes D(\beta)(\sigma_{in}^T \otimes |\alpha\rangle\langle\alpha|)D^\dagger(\beta) \otimes D^\dagger(\beta)$. Using the invariance $d^2\beta = d^2(\beta + \alpha)$, $\forall\alpha$, and similar methods to those in Ref. [46], we find that

$$\mathbf{O}_F = \sum_{K=0}^{\infty}\sum_{i,j=0}^{K}\frac{1}{2^{K+1}}\sqrt{\binom{K}{i}\binom{K}{j}}|i,j\rangle\langle K-j, K-i|. \quad (38)$$

Moreover, by noticing that the partially transposed $\mathbf{O}_F^\Gamma$ is block diagonal, we can simplify the fidelity (37) as follows,

$$F = \frac{\text{Tr}[\rho_{AB}^{\Gamma_A}\mathbf{O}_F^\Gamma]}{\text{Tr}(\rho_{AB}^{\Gamma_A})} = \frac{\sum_{K=0}^{\infty}\text{Tr}[\mathbf{C}_K\mathbf{O}_F^\Gamma(K)]}{\sum_{K=0}^{\infty}\text{Tr}[\mathbf{C}_K]}, \quad (39)$$

where $\mathbf{O}_F^\Gamma(K)$ is the K sub-block matrix $\langle i|\mathbf{O}_F^\Gamma(K)|j\rangle = \langle i, K-i|\mathbf{O}_F^\Gamma|j, K-j\rangle$.

Thus, using $\mathbf{C}_K$ as defined above, the teleportation fidelity can be easily evaluated. For example, for the state before
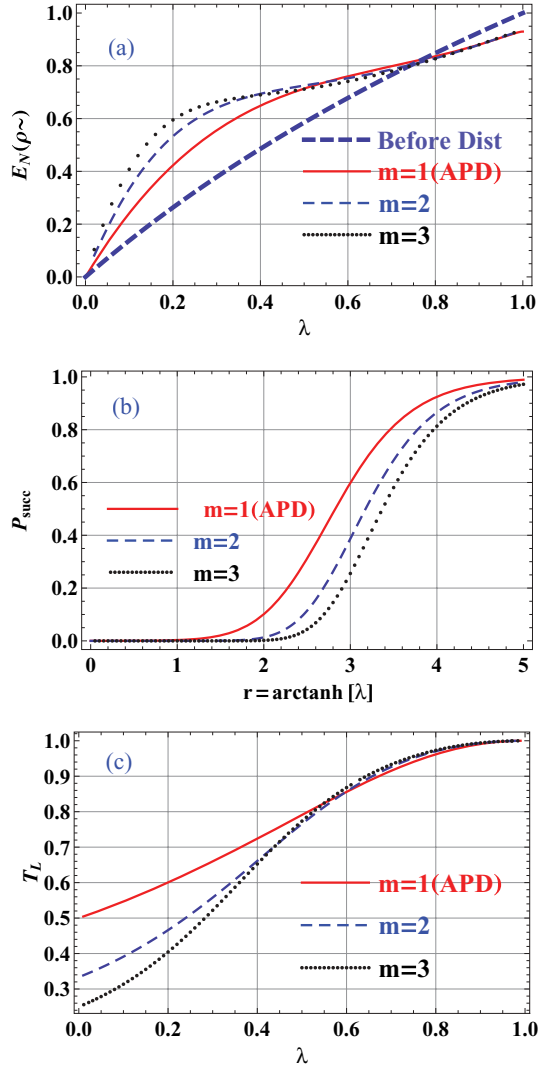
FIG. 7. (Color online) Logarithmic negativity (a) and success probability (b) for the mixed PNR method (strategy 2) with $m = 1$, $m = 2, m = 3$. The lower bound T_L (c) varies from $1/(m + 1)$ to 1; the other parameters are chosen as $\eta = 1/2, T = 0.95$.

entanglement distillation, the matrix $\mathbf{C}_K$ is given by Eq. (8), and the fidelity becomes

$$
\begin{aligned}
F_{\mathrm{mix}} &= \sum_{K=0}^{\infty} \sum_{i,j=0}^{K} C_{i,j}^{(K)} \langle i|\mathbf{O}_{\mathrm{F}}^{\Gamma}|j\rangle \\
&= \frac{(1+\lambda)(2 - \lambda^3 \eta^3 + \lambda^2 \eta^2 (\lambda + 3) - \lambda \eta (\lambda + 4))}{2(2 - 2\lambda\eta - \lambda^2 \eta + \lambda^2 \eta^2)(1 - \lambda\eta)(1 + \lambda - \lambda\eta)}.
\end{aligned}
\tag{40}
$$

Similarly, from the definitions in Eqs. (20) and (28), the teleportation fidelity for the PS-distilled states can be obtained, respectively. For example, in comparison with the logarithmic negativities calculated in Sec. V, we present a numerical evaluation of the teleportation fidelity for pure PNR-distilled entangled states in Fig. 8. For $\ell = 1, 2, 3$, the teleportation fidelity is obviously improved in the low-squeezing regime ($\lambda \lesssim 0.75$), in a similar way to what we obtained for the logarithmic-negativity measured entanglement in Fig. 5. However, note
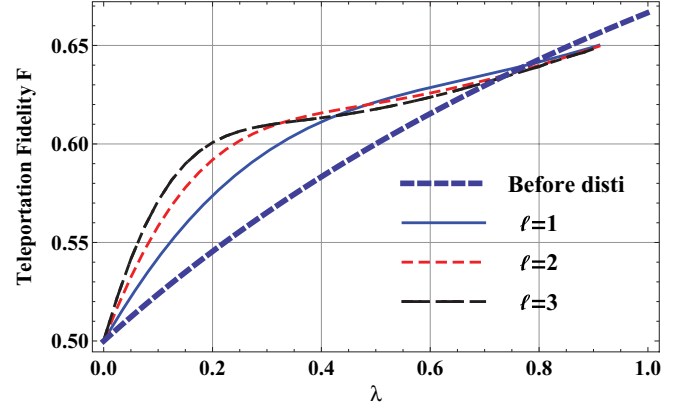
FIG. 8. (Color online) Fidelity of teleporting an unknown coherent state $\sigma_{\mathrm{in}} = |\alpha\rangle\langle\alpha|$ using a pure-PNR-distilled amplitude-damped TMSS. The parameters are $\eta = 1/2, T = 0.95$ as in Fig. 5.

that the logarithmic negativity is known to have an operational meaning (quantified by the quality of quantum correlations used in quantum teleportation) only for symmetric Gaussian states. Indeed, our amplitude-damped TMSSs do belong to the class of symmetric Gaussian states. However, for the photon-subtracted, non-Gaussian states after distillation, the correspondence between logarithmic negativity and coherent-state teleportation fidelity is not obvious; even though it is possible to relate the second-moment correlations of photon-subtracted states with their logarithmic negativities [47].

VII. CONCLUSIONS

In conclusion, we have studied a photon-subtraction-based entanglement distillation scheme on a single copy of a Gaussian mixed state in form of an amplitude-damped TMSS using beam splitters and various photon detection strategies. The photon measurements included on-off and photon number resolving detectors, as well as mixed photon number resolving detections where the on-off threshold can be varied compared to the conventional on-off measurement with zero or nonzero photons detected. Exploiting the symmetry and centrosymmetry properties of the partially transposed density matrix written in the Fock basis, we were able to derive explicit formulas for the entanglement of the non-Gaussian mixed states after distillation in terms of the logarithmic negativity.

We showed that in order to improve the entanglement after the imperfect channel transmission of the TMSS subject to photon losses, a constraint represented by a lower bound for the beam splitters (used for photon subtraction) must be satisfied. Our results extend earlier work on continuous-variable distillation from pure entangled states to the more general case of mixed entangled states, as one usually encounters in most realistic situations such as experimental demonstrations [18] and optical-fiber-based communications. Most importantly, even for channel attenuations as large as 3 dB, the photon-subtraction-based entanglement distillation scheme still works fairly well, provided the input squeezing is chosen sufficiently small.

The applicability of our protocol to actual long-distance quantum communication, for instance, by building up a quantum repeater [32], depends on various parameters. First,

note that the success probabilities in the present scheme are rather low; i.e., as low as or even lower than those of the known discrete-variable repeater proposals based on single-photon detections. Moreover, our results show that for any (sufficiently small) initial squeezing λ for which the distilled entanglement exceeds the input entanglement, there is always a different, effective squeezing value $\lambda_{\text{eff}} > \lambda$ for which the same or even higher entanglement can be distributed through the lossy channels without subsequent distillations. This suggests that our distillation still mainly functions as an entanglement concentration, similar to what can be obtained for photon-subtraction-based distillation of pure states. It is important to see that distillation still works for mixed states; however, in a potential application, it may still be better to use large squeezing from the beginning without distillation. In this case, the question arises how large this input squeezing must be to beat the distillation-based protocol.

More specifically, using our formulas, one can find that the logarithmic negativities before and after distillation are related by $\lim_{\lambda \to 1} E_N^{\text{before}}(\eta,\lambda) > E_N^{\text{after}}(\eta,\lambda_0,T)$, for all initial squeezings λ_0, all channel transmissions η, and all photon-subtraction transmittances $T < 1$. Nonetheless, for example, with 3-dB losses in the channel (corresponding to an elementary distance in a quantum repeater of almost one attenuation length), the same entanglement as for transmitting an almost 10-dB-squeezed TMSS without distillation can be obtained through photon-subtraction-based distillation of a roughly 6-dB-squeezed TMSS after transmission. However, the former approach would be deterministic, whereas the latter is highly probabilistic, leading to further complications in a full quantum repeater such as the need for sufficient quantum memories. Further extensions of our scheme, including more general measurements and local operations on a single Gaussian mixed state or multicopy distillations may prove superior to the protocol presented here.

ACKNOWLEDGMENTS

[1] A. Einstein, B. Podolsky, and N. Rosen, Phys. Rev. **47**, 777 (1935).

[2] S. L. Braunstein and P. van Loock, Rev. Mod. Phys. **77**, 513 (2005).

[3] J. Eisert and M. Plenio, Int. J. Quantum. Inf. **1**, 479 (2003).

[4] G. Adesso and F. Illuminati, J. Phys. A: Math. Theor. **40**, 7821 (2007).

[5] C. H. Bennett, H. J. Bernstein, S. Popescu, and B. Schumacher, Phys. Rev. A **53**, 2046 (1996).

[6] P. G. Kwiat, S. Barraza-Lopez, A. Stefanov, and N. Gisin, Nature (London) **409**, 1014 (2001).

[7] J. W. Pan, C. Simon, Č. Brukner, and A. Zeilinger, Nature (London) **410**, 1067 (2001).

[8] T. Yamamoto, M. Koashi, Ş. K. Özdemir, and N. Imoto, Nature (London) **421**, 343 (2003).

[9] R. Reichle *et al.*, Nature (London) **443**, 838 (2006).

[10] J. Eisert, S. Scheel, and M. B. Plenio, Phys. Rev. Lett. **89**, 137903 (2002).

[11] J. Fiurášek, Phys. Rev. Lett. **89**, 137904 (2002).

[12] G. Giedke and J. I. Cirac, Phys. Rev. A **66**, 032316 (2002).

[13] T. Opatrný, G. Kurizki, and D. G. Welsch, Phys. Rev. A **61**, 032302 (2000).

[14] M. S. Kim, E. Park, P. L. Knight, and H. Jeong, Phys. Rev. A **71**, 043805 (2005).

[15] S. Olivares, M. G. A. Paris, and R. Bonifacio, Phys. Rev. A **67**, 032314 (2003).

[16] A. Kitagawa, M. Takeoka, M. Sasaki, and A. Chefles, Phys. Rev. A **73**, 042310 (2006).

[17] M. Sasaki and S. Suzuki, Phys. Rev. A **73**, 043807 (2006).

[18] H. Takahashi, J. S. Neergaard-Nielsen, M. Takeuchi, M. Takeoka, K. Hayasaka, A. Furusawa, and M. Sasaki, Nat. Photon. **4**, 178 (2010).

[19] P. van Loock, Laser Photonics Rev. [http://onlinelibrary.wiley.com/doi/10.1002/lpor.201000005/abstract].

[20] N. Gisin, Phys. Lett. A **210**, 151 (1996).

[21] A. Kent, N. Linden, and S. Massar, Phys. Rev. Lett. **83**, 2656 (1999).

[22] F. Verstraete, J. Dehaene, and B. DeMoor, Phys. Rev. A **64**, 010101(R) (2001).

[23] Zhi-Wei Wang, Xiang-Fa Zhou, Yun-Feng Huang, Yong-Sheng Zhang, Xi-Feng Ren, and Guang-Can Guo, Phys. Rev. Lett. **96**, 220505 (2006).

[24] J. Wenger, R. Tualle-Brouri, and P. Grangier, Phys. Rev. Lett. **92**, 153601 (2004).

[25] A. Ourjoumtsev, R. Tualle-Brouri, J. Laurat, and P. Grangier, Science **312**, 83 (2006).

[26] V. Parigi, A. Zavatta, M. S. Kim, and M. Bellini, Science **317**, 1890 (2007).

[27] J. Fiurášek, Ladislav Mišta Jr., and R. Filip, Phys. Rev. A **67**, 022304 (2003).

[28] D. E. Browne, J. Eisert, S. Scheel, and M. B. Plenio, Phys. Rev. A **67**, 062320 (2003).

[29] A. P. Lund and T. C. Ralph, Phys. Rev. A **80**, 032309 (2009).

[30] L.-M. Duan, G. Giedke, J. I. Cirac, and P. Zoller, Phys. Rev. Lett. **84**, 4002 (2000).

[31] S. Rebic, S. Mancini, G. Morigi, and D. Vitali, J. Opt. Soc. Am. B **27**, A198 (2010).

[32] H.-J. Briegel, W. Dür, J. I. Cirac, and P. Zoller, Phys. Rev. Lett. **81**, 5932 (1998).

[33] G. Vidal and R. F. Werner, Phys. Rev. A **65**, 032314 (2002).

[34] M. B. Plenio, Phys. Rev. Lett. **95**, 090503 (2005).

[35] J. Eisert, Ph.D. thesis, University of Potsdam, 2001.

[36] Phoenix S. Y. Poon and C. K. Law, Phys. Rev. A **76**, 012333 (2007).

[37] A. Cantoni and P. Butler, Linear Algebra Appl. **13**, 275 (1976).

[38] C. W. Helstrom, *Quantum Detection and Estimation Theory* (Academic Press, New York, 1976).

[39] A. S. Holevo, *Probabilistic and Statistical Aspects of Quantum Theory* (North-Holland, Amsterdam, 1982).

[40] E. Knill, R. Laflamme, and G. J. Milburn, Nature (London) **409**, 46 (2001).

[41] C. Simon, H. de Riedmatten, M. Afzelius, N. Sangouard, H. Zbinden, and N. Gisin, Phys. Rev. Lett. **98**, 190503 (2007).

[42] C. Wittmann, U. L. Andersen, M. Takeoka, D. Sych, and G. Leuchs, Phys. Rev. Lett. **104**, 100505 (2010).

[43] I. Afek, O. Ambar, and Y. Silberberg, Phys. Rev. Lett. **104**, 123602 (2010).

[44] I. Afek, A. Natan, O. Ambar, and Y. Silberberg, Phys. Rev. A **79**, 043830 (2009).

[45] S. L. Braunstein and H. J. Kimble, Phys. Rev. Lett. **80**, 869 (1998).

[46] Ladislav Mišta Jr., Phys. Rev. A **73**, 032335 (2006).

[47] G. Adesso, Phys. Rev. A **79**, 022315 (2009).